

ELECTRON EMISSION PROPERTIES OF Si FIELD EMITTER ARRAYS COATED WITH NANOCRYSTALLINE DIAMOND FROM FULLERENE PRECURSORS

T.G. McCauley¹, T.D. Corrigan^{1,2}, A.R. Krauss¹, O. Auciello³, D. Zhou¹, D.M. Gruen¹,
D.Temple⁴, R.P.H. Chang², S. English⁵, and R.J. Nemanich⁵

¹ Materials Science and Chemistry Divisions, Argonne National Laboratory, Argonne, IL 60439

² Department of Materials Science and Engineering, Northwestern University, Evanston, IL 60208

³ Materials Science Division, Argonne National Laboratory, Argonne, IL 60439

⁴ Electronics Technology Division, MCNC, Research Triangle Park, NC 27709

⁵ Department of Physics, North Carolina State University, Raleigh, NC 27695

ABSTRACT

In this paper, we report on a substantial lowering of the threshold field for electron field emission from Si field emitter arrays (FEA), which have been coated with a thin layer of nanocrystalline diamond by microwave plasma-assisted chemical vapor deposition (MPCVD) from fullerene (C₆₀) and methane (CH₄) precursors. The field emission characteristics were investigated and the emission sites imaged using photoelectron emission microscopy (PEEM). Electron emission from these Si FEAs coated with nanocrystalline diamond was observed at threshold fields as low as 3 V/ μ m, with effective work functions as low as 0.59 eV.

INTRODUCTION

Flat panel displays (FPDs) based on field emitter arrays have several potential performance advantages over present displays utilizing active matrix liquid crystal display (AMLCD) technology. The advantages of field emission displays (FEDs) include higher brightness, a wider range of viewing angles, and lower power requirements [1, 2]. Silicon microtip arrays are attractive because they are readily fabricated using conventional techniques. Several types of low-work function coatings, including diamond, have been investigated for Si FEAs [1, 3, 4, 5].

Previous attempts to coat Si emitter tips with diamond by conventional CH₄/H₂ CVD growth processes have been only partially successful. In some cases a lowering of the threshold field and/or effective work function have been observed [3, 4, 5]. However, no one has yet demonstrated the ability to conformally coat a field emitter tip with a diamond layer which is sufficiently thin that the tip geometry and radii are not significantly modified. In this paper we report on the electron emission characteristics of Si FEAs coated with very thin nanocrystalline diamond films from fullerene and methane precursors in an Ar-rich microwave discharge.

EXPERIMENTAL

The MPCVD (2.45 GHz) deposition system in which the diamond films were prepared is a modified ASTeX PDS-17 CVD reactor. The process gases used were Ar, H₂, CH₄, and N₂. For the depositions using C₆₀ as a precursor, 80 sccm of Ar gas was flowed through a quartz tube furnace containing mixed fullerene soot. The furnace temperature was adjusted to give a partial pressure of carbon in the deposition chamber approximately equivalent to ~0.5 Torr of CH₄. The Ar carried sublimed C₆₀ molecules through a 1 μ m filter and into the deposition chamber via a heated injection nozzle positioned ~1 cm above the substrate. Further details of the sublimation

source are given elsewhere [6, 7]. The (100) n-type Si substrates were pretreated using bias-enhanced nucleation (BEN). The bias voltage, V_b , and time, t_b , are shown in the table below, as are the substrate temperature, T_{sub} , and threshold field for electron emission (where observed), E_{FE} .

Table I: *Bias and Growth Conditions for Diamond Coating of Si FEAs*

Chemistry	V_b (V)	t_b (min)	t_{growth} (hr)	T_{sub} ($^{\circ}$ C)	E_{FE} (V/ μ m)	Notes
1. $C_{60}/H_2/Ar$	-120	60	0.50	800	2.9	1, 3
2. $C_{60}/H_2/Ar$	-160	36	1.10	800	5.0	1, 3
3. $C_{60}/H_2/Ar$	-160	40	1.15	800	3.2	1, 3
4. $CH_4/N_2/Ar$	-100	15	0.5	800	10	2, 4
5. $CH_4/N_2/Ar$	-100	15	1.0	800	5.0	2, 4
6. $CH_4/N_2/Ar$	-100	15	2.0	800	-	2, 4

¹BEN: 10% $CH_4/90\%$ H_2 , 50 sccm total flow, total pressure 5 Torr, 500 W.

²BEN: 5% $CH_4/95\%$ H_2 , 50 sccm total flow, total pressure 10 Torr, 500 W.

³Growth: $C_{60}/20\%$ $H_2/80\%$ Ar, 100 sccm total flow, total pressure 100 Torr, 800 W.

⁴Growth: 1% $CH_4/2\%$ $N_2/97\%$ Ar, 100 sccm total flow, total pressure 100 Torr, 800 W.

Micro-Raman and XRD spectra from the films confirmed the phase purity of both the $C_{60}/H_2/Ar$ and the $CH_4/N_2/Ar$ films. A high resolution electron microscope with a field emission source (FESEM) was used to study the morphology and conformality of the coatings on the FEAs.

A schematic of the I-V field emission testing apparatus is shown in Figure 1. Typical vacuum base pressure during data acquisition was $\sim 10^{-8}$ Torr. The positively biased stainless steel anode was 2 mm in diameter. A typical probe-sample distance for testing a coated FEA was 100 μ m. A photoelectron emission microscope (PEEM) was used to image the emission sites on the arrays after coating. The applied field was a constant at 10 V/ μ m (20 kV with a fixed sample distance of 2 mm). UV photoexcitation was provided by a filtered mercury arc lamp [8].

RESULTS AND DISCUSSION

High resolution electron micrographs of the coated FEAs are shown in Figure 2. Figure 2a shows a single tip from sample 1 (see Table I). The thickness of the coating over the regions where it is continuous is ~ 600 \AA . Unlike sample 2, sample 3 was hydrogen plasma-treated prior to BEN. The effect of the pre-BEN etching in a hydrogen plasma was to roughen the sample surface on a nanometer scale, thus providing an extremely high density of potential nucleation sites. The result is the ~ 600 \AA thick conformal coating shown in Figure 2b. Figure 2c shows the formation of a cluster on vertically-oriented 'nanotips' on the apical surface of a tip as well as the discontinuous coverage of the shank and base plane (sample 2). The array whose emitter tips were topped with these 'nanotips' proved to have a lower threshold field for electron emission than the continuous, conformally coated array. Figure 2d shows a discontinuous coating, from a $CH_4/N_2/Ar$ microwave plasma, on sample 4. Here the coating appears to have modified the apical surface and tip radius.

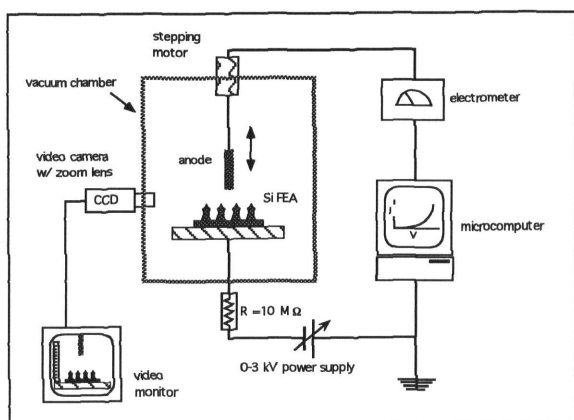


Figure 1. Schematic of electron field emission testing system with variable anode-sample distance.

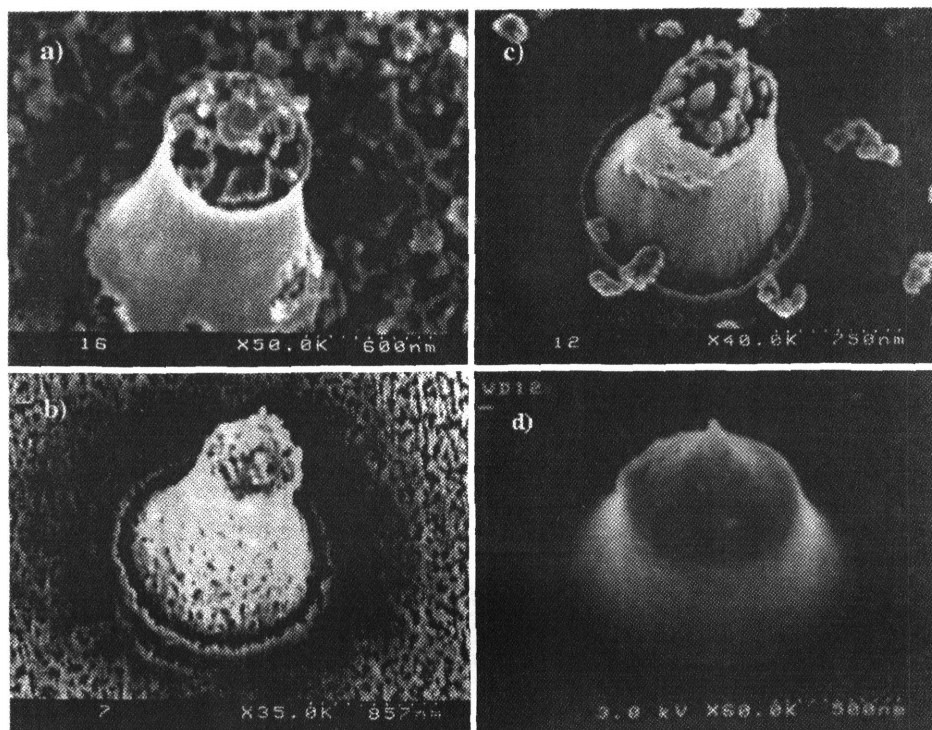


Figure 2. FESEM micrographs of (a) discontinuous and, (b) conformal coatings, and (c) nanotips on a single tip, all from $C_{60}/20\% H_2/80\% Ar$. Panel (d) shows a discontinuous N-incorporated film deposited on a single tip from $1\% CH_4/2\% N_2/97\% Ar$.

Figure 3a shows I-V curves for the Si FEAs coated with nanocrystalline diamond from $C_{60}/20\% H_2/80\% Ar$, while figure 3b shows the Fowler-Nordheim (F-N) plot for the continuous, conformally coated FEA (sample (2), see Fig. 2b). From the F-N plot for emission from an uncoated Si FEA, the geometrical field enhancement factor, β , for these tip arrays was found to be ~ 185 . Note that the threshold field for emission from an uncoated FEA was $\sim 40 V/\mu m$. The discontinuous, conformally coated FEA (sample (1), see Fig. 2a) exhibited the lowest threshold field ($2.9 V/\mu m$) and effective work function ($\phi=0.71 eV$ for $\beta=185$). The FEA with the nanotip structures (sample (3), see Fig. 2c) showed a very similar threshold field ($3.2 V/\mu m$), and a slightly lower effective work function ($\phi=0.59 eV$ for $\beta=185$). The continuous, conformally coated FEA (sample (2), see Fig. 2b) emitted at a threshold field of $5.0 V/\mu m$, with an effective work function $\phi=1.21 eV$ for $\beta=185$. The FEAs coated with nitrogen-incorporated nanocrystalline diamond (samples (4) and (5), see Fig. 2d) showed threshold fields of 10 and $5.0 V/\mu m$, respectively, as shown in Figure 4a. The corresponding effective workfunctions for these coated FEAs were $\phi=2.22$ and $0.72 eV$, respectively, for $\beta=185$.

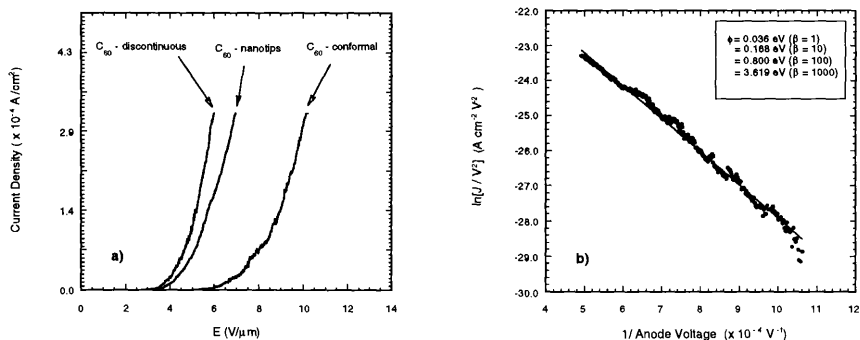


Figure 3. Field emission characteristics of nanocrystalline diamond-coated FEAs. (a) Current density vs. applied electric field for all three FEAs coated using $C_{60}/20\% H_2/80\% Ar$. (b) Fowler-Nordheim plot of field emission from the conformally and continuously coated FEA (' C_{60} - conformal' in Figure 3a) shown in Figure 2b.

The reduction in threshold field for emission for both $C_{60}/Ar/H_2$ - and $CH_4/Ar/N_2$ -coated FEAs, relative to an uncoated array, is shown clearly in Figure 4a. Figure 4b shows the dependence of the effective work function on the assumed value of β . From Figure 4b, using $\beta=185$, the reduction in the effective work functions of the $C_{60}/Ar/H_2$ - and $CH_4/Ar/N_2$ -coated FEAs was 3.6 - $4.2 eV$ and 2.6 - $4.1 eV$, respectively.

The PEEM images in Figure 5 show that the emission from the nitrogen-incorporated nanocrystalline diamond-coated Si FEAs is highly uniform and originates from the coated tips. It should be noted that the coated samples were transported in air from the growth and field emission testing facility to the remote site of the PEEM analysis facility. Upon initial insertion into the PEEM microscope, electron emission from the FEA was observed only with UV illumination. After a one minute *in-situ* H_2 plasma treatment (1 Torr, 20 W rf power), pure field emission was observed. That is, low-threshold electron emission in the absence of UV illumination.

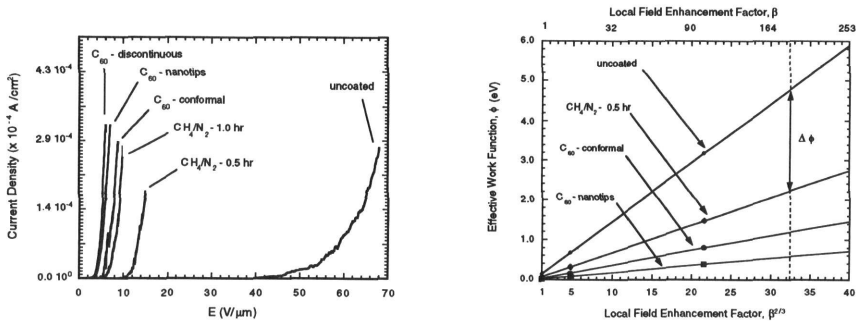


Figure 4. Field emission characteristics of nanocrystalline diamond-coated FEAs. (a) Current density vs. applied electric field for all FEAs coated using both $C_{60}/80\% \text{ Ar}/20\% \text{ H}_2$ and $1\% \text{ CH}_4/97\% \text{ Ar}/2\% \text{ N}_2$, and (b) a plot of the effective work function, ϕ , vs. the local field enhancement factor, β , showing the apparent reduction in ϕ due to diamond coating from $C_{60}/\text{Ar}/\text{H}_2$ and $\text{CH}_4/\text{Ar}/\text{N}_2$, at each value of β .

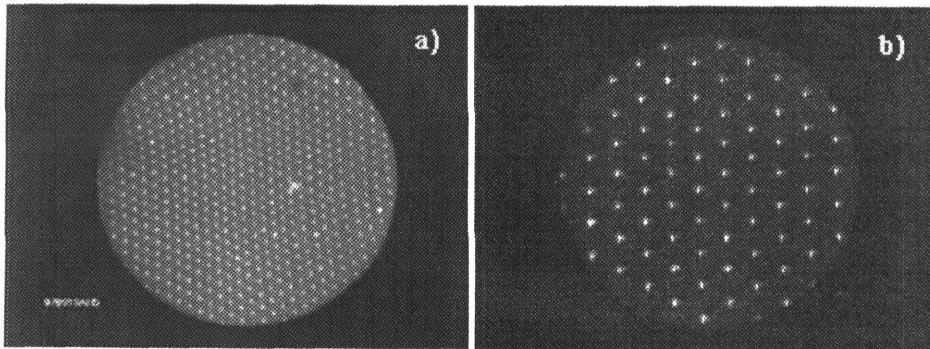


Figure 5. PEEM images of Si FEA with nitrogen-incorporated nanocrystalline diamond coating from $1\% \text{ CH}_4/97\% \text{ Ar}/2\% \text{ N}_2$ microwave plasma. Shown here with UV illumination at (a) low magnification, $150 \mu\text{m}$ field of view, and (b) higher magnification, $50 \mu\text{m}$ field of view. Note the high uniformity of emission over the entire field of view.

The images shown in Figure 5 were taken after the hydrogen treatment and with UV illumination. PEEM analysis of the FEAs coated from a $C_{60}/20\% \text{ H}_2/80\% \text{ Ar}$ plasma is in progress at the time of this writing.

CONCLUSIONS

In conclusion, this work demonstrates our ability to coat array structures with thin ($\sim 600 \text{ \AA}$), conformal, continuous films of phase-pure nanocrystalline diamond. The film thickness and degree of coverage do appear to be issues, however FESEM and field emission analysis indicate that, beyond some minimal degree of coverage, local modification of emitter tip geometry is more critical than conformality of the diamond coating.

Si FEAs coated with nanocrystalline diamond from a $C_{60}/Ar/H_2$ microwave plasma, exhibited a reduction in threshold field for electron emission from $>40 \text{ V}/\mu\text{m}$ to $\sim 3 \text{ V}/\mu\text{m}$. Si FEAs coated with nitrogen-incorporated nanocrystalline diamond from a $CH_4/Ar/N_2$ microwave plasma, exhibited a reduction in threshold field for electron emission from $>40 \text{ V}/\mu\text{m}$ to $\sim 5 \text{ V}/\mu\text{m}$. All samples studied exhibit highly linear Fowler-Nordheim plots, confirming that field emission is the sole mechanism responsible for the observed electron emission. The effective work functions of the $C_{60}/Ar/H_2$ -coated FEAs, derived from the Fowler-Nordheim plots using $\beta=185$, were $\phi=0.71$, 1.22 , and 0.59 eV for samples 1, 2, and 3, respectively. For the and $CH_4/Ar/N_2$ -coated FEAs, the effective work functions were $\phi=2.22$ and 0.72 eV for samples 4 and 5, respectively.

PEEM analysis shows that the emission from the nitrogen-incorporated nanocrystalline diamond-coated Si FEAs is highly uniform and that the emission originates from the emitter tips rather than the base plane. The emission current density from these FEAs is of the proper order ($\sim 1 \text{ mA}/\text{cm}^2$) for device applications such as FEDs [2].

ACKNOWLEDGMENTS

This work is supported by the U.S. Department of Energy, BES-Materials Sciences, under Contract W-31-109-ENG-38.

REFERENCES

1. A.A. Talin, T.E. Felter, and D.J. Devine, *J. Vac. Sci. Technol. B* **13**(2), 448 (1995).
2. G.R. Brandes, in *Handbook of Industrial Diamonds and Diamond Films*, ed. by M.A. Prelas, G. Popovici, and L.K. Bigelow (Marcel Dekker, New York, 1998), pp. 1103-1127.
3. H.C. Cheng, T.K. Ku, B.B. Hsieh, S.H. Chen, S.Y. Leu, C.C. Wang, C.F. Chen, I.J. Hsieh, and J.C. Huang, *Jpn. J. Appl. Phys.* **34**(I, 12B), 6926 (1995).
4. E.I. Givargizov, V.V. Zhirnov, A.N. Stepanov, P.S. Plekhanov, and R.I. Kozlov, *Appl. Surf. Sci.* **94-5**, 117 (1996).
5. E.I. Givargizov, L.L. Aksenova, A.V. Kuznetsov, P.S. Plekhanov, E.V. Rakova, A.N. Stepanova, V.V. Zhirnov, and P.C. Nordine, *Diam. Relat. Mat.*, **5**(9), 938 (1996).
6. D.M. Gruen, S. Liu, A.R. Krauss, and X. Pan, *J. Appl. Phys.* **75**(3), 1758 (1994).
7. D.M. Gruen, C.D. Zuiker, A.R. Krauss, and X. Pan, *J. Vac. Sci. Technol. A* **13**(3), 1628 (1995).
8. W.N. Unertl and M.E. Kordesch, in *Handbook of Surface Science Vol. 1: Physical Structure*, ed. by W.N. Unertl (Elsevier, Amsterdam, 1996), pp. 361-421.